Chemical Engineering & Processing: Process Intensification 160 (2021) 108251

Contents lists available at ScienceDirect

Chemical Engineering and Processing - Process Intensification

journal homepage: www.elsevier.com/locate/cep

Twisted architecture for enhancement of passive micromixing in a wide range of Reynolds numbers

Shima Akar [a,b,c], Amin Taheri [a,b,c], Razavi Bazaz [d], Ebrahimi Warkiani [d], Mousavi Shaegh [a,b,c,*]

[a] Orthopedic Research Center, Mashhad University of Medical Sciences, Mashhad, Iran
[b] Clinical Research Unit, Ghaem Hospital, Mashhad University of Medical Sciences, Mashhad, Iran
[c] Laboratory of Microfluidics and Medical Microsystems, BuAli Research Institute, Mashhad University of Medical Sciences, Mashhad, Iran
[d] School of Biomedical Engineering, University of Technology Sydney, New South Wales, Australia

ARTICLE INFO

Keywords:
Dean vortices
Micromilling
Microfluidics
Twisted structure
Passive micromixer

ABSTRACT

Micromixers present essential roles in providing homogeneous mixtures in microfluidic systems. It is of critical importance to introduce strategies to increase the mixing efficiency of passive micromixers, capable of operating at high efficiency levels over a wide range of Reynolds (Re) numbers. To this end, a novel design of twisted microstructure for enhancing mixing performance in a wide range of Reynolds numbers was introduced. Incorporating this microstructure with straight and serpentine micromixers was numerically and experimentally investigated. Micromixers with twisted microstructures were fabricated in Poly(methyl methacrylate) (PMMA) using high-precision micromilling. The effects of Reynolds number, pitch number, and channel hydraulic diameter on mixing efficiency and pressure drop were analyzed. Results revealed that the twist architecture could increase mixing efficiency significantly with very low pressure drop of up to 0.89 kPa. The twisted serpentine micromixer could narrow the disparity of mixing efficiency from 87% (Re = 10) to 98% (Re = 400). High mixing efficiency could be achieved within a length of 4.8 mm in the twisted serpentine micromixer with a hydraulic diameter of 300 μm. Taken together, the twisted structure could be incorporated with various geometries to create compact and high efficiency micromixers for operation in a wide range of Re numbers.

1. Introduction

In recent years, microfluidics has become increasingly widespread, as evidenced by countless applications in biomedical, chemical, and pharmaceutical realms. These platforms proffer superior advantages over conventional macroscale methods. In microfluidic devices, often, two or more samples mix together, followed by analyzing in downstream. Micromixers are widely employed in microfluidic systems to produce homogenous mixtures for chemical reaction [1], chemical synthesis [2], purification [3], polymerization [4], sample pre-concentration [5], DNA digestion [6], and nanomedicine [7]. Mixing in such applications is of critical importance since heterogeneous mixing has negative impacts on the features of the final products. In microfluidic devices, mixing is usually restricted by diffusion, which is relatively prolonged and not efficient for downstream analysis [8]. To this end, the enhancement of mixing efficiency has been the focus of various investigations.

In general, mixing processes could be modulated through two main groups of passive and active [9]. In active micromixers, the mixing process is enhanced through using an external actuation such as a magnetic field [10], ultrasonic vibration [11,12], electrical field [13,14], and electrothermal force [15,16]. Despite the degree of mixing efficiency, active micromixers are costly and more complex to fabricate and integrate with other components of a microfluidic system. Moreover, the use of an external force may induce undesired impacts on some reagents and biological samples. Alternatively, passive micromixers have been extensively used in microfluidic devices owing to their valuable benefits such as simple to integrate, cost-effective to produce, and no requirement for using any external power supply [8]. Passive micromixers are mainly classified based on (i) mixing mechanism or (ii) their microstructure. The mixing mechanism could be sub-classified into chaotic advection and molecular diffusion, while the mixing microstructures could be mainly categorized into two major subgroups to produce lamination or rotation in flow [17,18]. The lamination-based micromixers use multiple channels [19], obstacles within mixing region [20], and convergence-divergence channels to produce consecutive

* Corresponding author at: Orthopedic Research Center, Mashhad University of Medical Sciences, Mashhad, Iran.
E-mail address: mousavisha@mums.ac.ir (M. Shaegh).

https://doi.org/10.1016/j.cep.2020.108251
Received 23 July 2020; Received in revised form 20 October 2020; Accepted 30 November 2020
Available online 28 December 2020

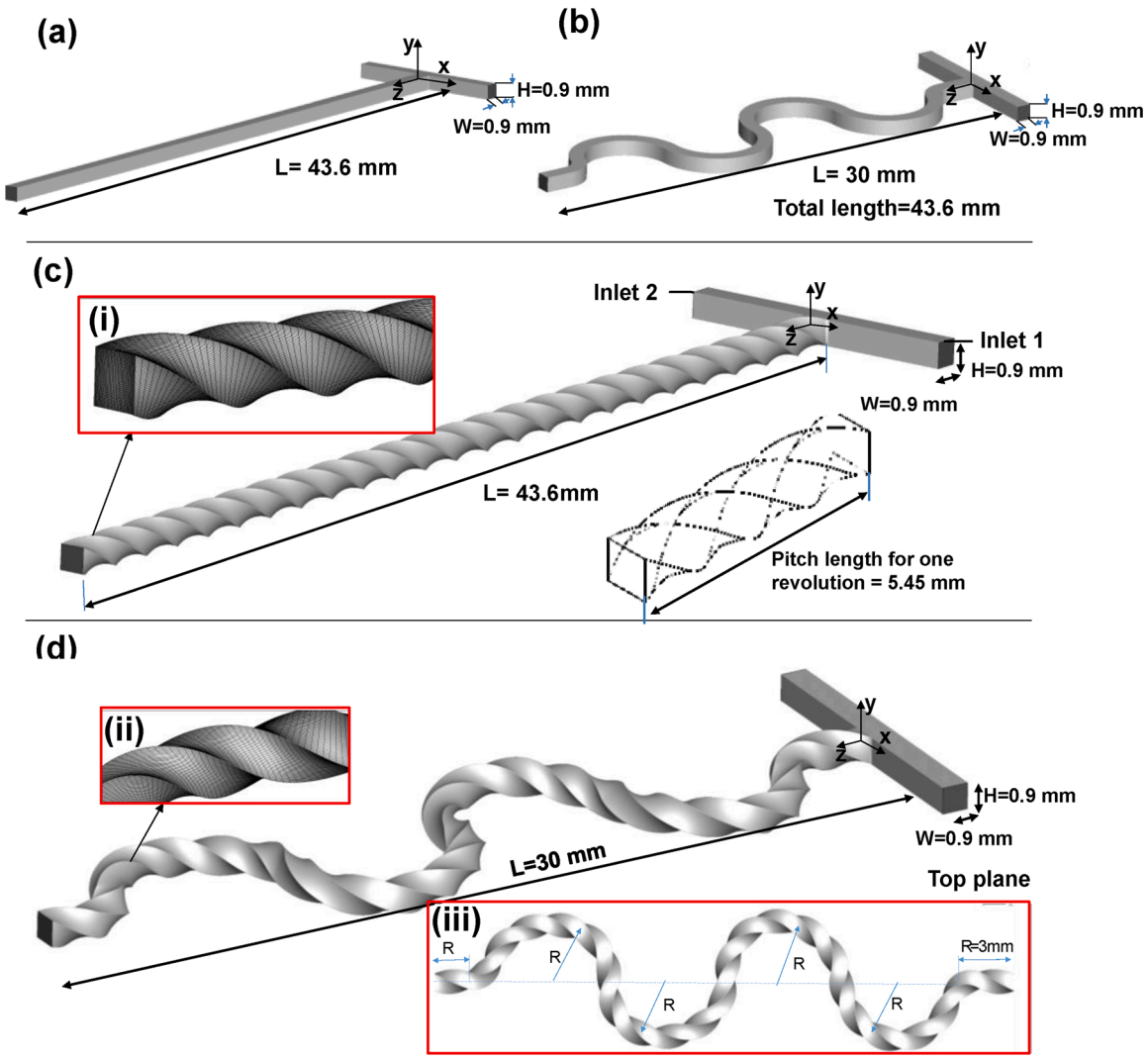

Fig. 1. The structure of the designed micromixers; (a) straight micromixer; (b) serpentine micromixer; (c) twisted straight micromixer at pitch number of 8; and (d) twisted serpentine mixer at pitch number of 8. Insets (i) and (ii) show the computational mesh used for flow analysis in the twisted straight and twisted serpentine micromixers, respectively. Inset (iii) shows the top plane of twisted serpentine micromixer.

separation and recombination (SAR) for enhancing mixing efficiency relying on diffusion mechanism.

Rotation-based micromixers with planar serpentine and spiral/helical geometries are more popular in use and provide higher mixing efficiency compared to lamination-based ones, by virtue of inducing transversal secondary flow and Dean vortices along mixing channel based on chaotic advection [21]. Generally, Dean vortices could be easily induced via curvatures [22]. Various micromixers based on Dean vortices have been proposed through the modulating of curved channel design. In one of the earliest studies, Liu et al. [23] experimentally assessed the performance of a 3D serpentine C-shaped passive micromixer for the Reynolds (Re) numbers from 6 to 70 and found that at the highest Re number, the serpentine micromixer, in order, had 16 times and 1.6 times higher performance than a straight and square-wave micromixer. With regard to improving the mixing efficiency by imposing more disturbance in flow lines, Li et al. [24] studied the performance of an S-shaped micromixer for Re numbers ranged from 2.5–30. As compared to a planar serpentine micromixer, their structure had 38% and 79% higher mixing performance at Re numbers of 5 and 30, respectively. It is clear that by increasing the number of curved channels and have a continuous curvature along the channel length, the mixing performance is improved. In this way, many investigations have shifted the attitude from single C-shaped and S-shaped geometries to spiral and periodic curved shapes.

Passive micromixers based on helical shape utilizing two curved square channels was firstly introduced by Schönfeld and Hardt [25]. Sudarsan and Ugaz [17] experimentally investigated five various spiral microchannel shapes with varying channel lengths at Re numbers ranged from 0.02–18.6. They concluded that the mixing performance could be improved by combining vortex effects with sudden changes through the flow path. They declared that the transverse Dean flows result in the mixing performance of over 90%. By comparing six different structures for Re numbers within the range of 0.1–100, Chen et al. [26] found that amongst of all considered structures, the square wave micromixer in moderate pressure drop had higher mixing efficiency. Duryodhan et al. [21] performed a three-dimensional numerical and experimental research on the performance of passive micromixers with T-, meander, and spiral shapes with different aspect ratios in the Re numbers range from 1 to 468. They observed that the mixing performance for aspect ratio of 1.2 and Re number of 140 was 100%, and this value for aspect ratio of 0.36 and Re number of 90 was roughly 74%. Although the rotation-based micromixers could provide high mixing efficiency, their high-performance operation could mainly occur in a narrow range of Re numbers. To accelerate the mixing process in Dean vortices-based micromixers at a wide range of flow rates, the idea of incorporating additional passive effects has been explored in several

studies. Liu et al. [27] analyzed the effect of SAR shape on dual helical micromixers at low Re numbers for the rapid mixing process. It was shown that mixing efficiency of 99% could be achieved for Re numbers within the range of 0.003–30 for channels with four loops. To take advantage of simultaneous diffusion mixing and Dean vortices-based mixing, Rafeie et al. [28] developed a new passive micromixer with lemniscate-shaped using 3D printing technology. High mixing efficiencies of more than 90% over a wide range of Re numbers from 1 to 1000 were obtained; however, high length (about 95 mm) and diameter (1.5 mm) of their micromixer may inhibit its deployment for many applications. For further mixing efficiency improvement, Jafari et al. [29] compared the performance of various passive twisted micromixers with plain microchannel to liquid-liquid extraction of water and kerosene for $76.7 \leq Re \leq 460.3$. They elucidate that by increasing the twist angle, both mixing efficiency and pressure drop were increased. Recently, Kang [30] carried out a 3D numerical study to assess the relative mixing cost and degree of mixing of micromixer with twisted structure in the range twist angle of $0-34\pi$ (0–17 revolutions) and low Re number range of 0.15−6. Based on their results, the mixing performance of twisted micromixer with 12 revolutions (twist angle of 24π) was 0.843, which was nearly four times higher than the straight channel.

In general, the reported schemes of passive micromixing require operation within a limited range of Re numbers to provide high mixing efficiency. Moreover, the currently available three-dimensional passive micromixers with high mixing efficiency within a wide range of Re number [28] induce high pressure drop and require costly fabrication methods such as high-precision 3D printing methods. In this study, a twisted microstructure was incorporated into straight and serpentine geometries to enhance mixing efficiency (>90%) over a wide range of Re numbers from 1 to 400. In this way, twisted straight and twisted serpentine micromixers were designed and fabricated using a high-precision micromilling machine in PMMA and were assembled and bonded through low-pressure thermal fusion bonding. Their performance was numerically and experimentally characterized and compared with conventional T-shape and serpentine micromixers at various pitch number, Re numbers, and hydrodynamic diameter. The twisted microstructure could enhance mixing in the straight micromixer by inducing flow rotation along its mixing channel, while the mixing was improved in the serpentine micromixer through induced Dean vortices. The proposed twisted design and fabrication method enables the development of high-performance micromixers in an easy and cost-effective method for various lab-on-chip applications.

2. Numerical study

In order to gain insight on the flow behavior and mixing performance of the proposed twist microstructures, a numerical analysis was established. The detailed description of the numerical modeling is as followed.

2.1. Micromixers geometry

The micromixers used in this study consisted of a two-inlet microchannel with a square cross-section with a hydraulic diameter of D_h. We have compared the effect of twist microstructure in micromixers by analyzing four micromixers, named as straight, serpentine, twisted straight, and twisted serpentine. Fig. 1 shows the computational domain, the coordinate system, and the dimension details of four different micromixers with pitch number (the number of revolution of the cross-section) of 8 (twist angle of 16π) in twisted micromixers. The length of the straight micromixers was considered equal to the total length of the serpentine micromixers.

2.2. Governing equations

It was assumed that the fluid flow was steady-state, incompressible, three dimensional (3D), and behaved as a Newtonian fluid with constant properties. With these assumptions, governing equations were presented as the following forms:

$$\nabla . \vec{V} = 0 \tag{1}$$

$$\rho\left[(\vec{V}.\nabla)\vec{V})\right] = -\nabla p + \mu\nabla^2\vec{V} \tag{2}$$

where $\vec{V}\left(\frac{m}{s}\right)$, $\rho\left(\frac{kg}{m^3}\right)$, $\mu(Pa{\cdot}s)$ and $p(Pa)$ are the velocity vector, density, dynamic viscosity, and pressure, respectively. Furthermore, the distribution of species concentration is described as follows:

$$\frac{\partial C}{\partial t} + (\vec{V}.\nabla)C = D\nabla^2 C \tag{3}$$

$C\left(\frac{mol}{m^3}\right)$ is the concentration of species, and $D(m^2/s)$ is the molecular diffusion coefficient of water.

The boundary conditions are defined as follows:

- Deionized water (DI) enters at inlet 1 having the following conditions:

$$\boldsymbol{u} = -\boldsymbol{u_{in}},\ \boldsymbol{v} = 0,\ \boldsymbol{w} = 0,\ \boldsymbol{C} = 1 \tag{4}$$

where u, v and w refer to velocity components in x, y and z directions, respectively.

- DI water enters at inlet 2 having the following conditions:

$$\boldsymbol{u} = \boldsymbol{u_{in}},\ \boldsymbol{v} = 0, \boldsymbol{w} = 0,\ \boldsymbol{C} = 0 \tag{5}$$

- Outlet: pressure outlet (static gauge pressure equal to zero)
- Micromixer channel wall: a stationary wall with no-slip condition (zero velocity)

2.3. Mixing efficiency

To evaluate the mixing efficiency of the micromixers, the mixing index (MI) of the species is defined as follows [31]:

$$\sigma = \sqrt{\frac{1}{M}\sum_{i=1}^{M}(c_i - \overline{c})^2} \tag{6}$$

$$\overline{c} = \frac{\sum_{1}^{m} c_i}{M} \tag{7}$$

$$MI = 1 - \sqrt{\frac{\sigma^2}{{\sigma_{max}}^2}} \tag{8}$$

In Eqs. (7) and (9), σ and σ_{max} denote the standard deviation and maximum variance of the mixture, respectively. M is the number of nodes inside the cross-section plane, c_i refers to the mass fraction of node i, $\overline{c}$ is the mass fraction at fully mixing region, which is equal to 0.5 in this study, and MI refers to the mixing index. The mixing index (MI) varies from 0 (0%, completely segregated state) to 1 (100%, homogeneously mixed state).

2.4. Numerical solution method

A numerical model was established in ANSYS Fluent 18.2 to investigate the fluid flow and mixing characteristics in the micromixer through the conservation Eqs. (1)–(3) with associated boundary conditions. It is worth mentioning that the SIMPLEC algorithm [32] was defined as a solution method for pressure-velocity coupling, and the

Table 1
The effects of grid number on mixing efficiency for straight twisted micromixer at Re = 100, P = 6.

Mesh size	MI (%)	Error (%)
256,000	78.3	9.2
404,300	71.7	4.9
864,800	68.3	1.01
1,523,000	69	

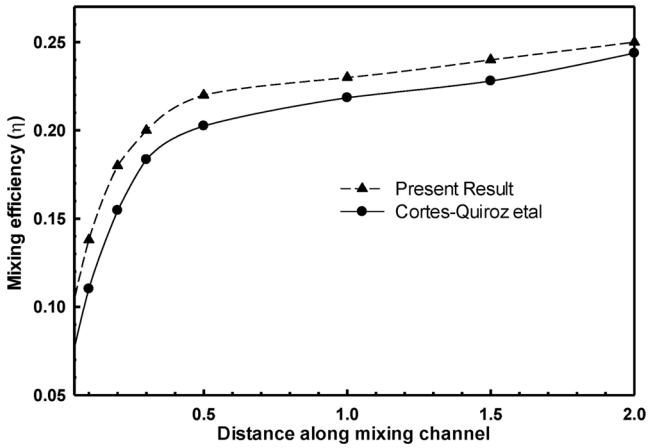

Fig. 2. The comparison of mixing efficiency of T-shape micromixer at Re = 150 with the results of the Cortes-Quiroz [33] study.

second-order upwind scheme was applied to discretize the continuity, momentum, and transport equation for species.

To investigate the grid-independency, the effect of four mesh numbers of 256,000, 404,300, 864,800, and 1,523,000 on the mixing efficiency (MI) of twisted straight micromixer was evaluated. As Table 1 reveals, beyond 864,800 elements, the effect of mesh numbers on the total performance of the mixer becomes negligible; therefore, the third mesh was adopted for the rest of the study. Fig. 1 shows that the mesh distribution is uniform with increasing the mesh density near the walls. Moreover, to validate the numerical model, the mixing efficiency of the T-shape micromixer was compared with the results of Cortes-Quiroz et al. [33], Fig. 2. The computational results are in close agreement with Cortes-Quiroz's findings, indicating that the numerical model has relatively high accuracy and reliability.

3. Fabrication process and mixing experiments

3.1. Materials and micromachining

Raw transparent Polymethyl Methacrylate (PMMA) sheets with a thickness of 4 mm were employed for the fabrication of the micromixers. The PMMA has high optical transparency and strong resistance to mechanical deformation. Meanwhile, PMMA could be easily processed with rapid prototyping methods, including laser micromachining [34,35] and high-precision micromilling [36,37] in a cost-effective manner with minimum investments. Furthermore, this polymer is biocompatible and has low toxicity, making it a proper material for some medical applications [38]. In this study, micromixers were fabricated in PMMA sheets using a commercially available micromilling CNC machine (DSP, China). Mastercam X7 software was employed to create CAM files for the micromilling process. The spindle speed, cutting speed, and feed rate in micromilling machine was set as 18,900 rpm, 75 m/min and 80 mm/min, respectively. The cutting tool was a micro carbide end mill for general use with a diameter of 0.3 mm, 2-flute AlTiNs coated 60 HRC. Fig. 3a illustrates the schematic of fabricated layers.

3.2. Surface treatment of micromilled channels

The surface of the twisted microchannels, fabricated through the micromilling process, was not smooth that might induce false results as appeared in the mixing performance. Thus, the microchannels were treated with chloroform to enhance their surface quality, as shown in Fig. 3b. For this aim, the micromilled channels were exposed to chloroform vapor at 40 ℃ for 3-4 min. Fig. 3c shows the surface topography obtained by a Scanning Electron Microscope (SEM) before and after the chloroform treatment.

3.3. Thermal fusion bonding

The fabricated PMMA specimens were assembled through the thermal fusion bonding process in two main stages. In the first stage, all PMMA specimens were washed using water-ethanol mixture and preheated at 90 ℃ and −80 kPa for 8 h in a vacuum oven, with subsequent cooling to room temperature in 30 min. In this way, the gas bubbles, trapped within the bulk of PMMA specimens, were released. This process was performed to enhance the bonding quality and optical transparency of the assembled layers [34]. In the second stage, the thermally treated layers were cleaned again with ethanol, and assembled between two glass slides and fixed with binder clips for heating at 130 ℃ and −80 kPa for 60 min. The workflow of the bonding process is shown in Fig. 3d and e.

3.4. Mixing characterization

Two micromixers with a pitch number of 8 and a diameter (D) of 0.9 mm were fabricated using the above-mentioned fabrication method. In the next step, the mixing test was performed with the use of yellow and blue food dye to justify the credibility of the numerical simulations at Re number of 10. Fig. 3f shows the experimental setup. Two solutions, comprised of 5 mL DI water containing 0.15 mL of food dye, were injected to the micromixer through the two inlets at the same flow of 208 $\mu L/min$, equivalent to Re = 10. Image acquisition was performed using an inverted microscope (TCM 400, Labomed, USA) coupled with a CCD camera (Labomed).

4. Results and discussion

4.1. Numerical simulation results

The main objective of this study was to propose novel micromixers with twisted architectures for high mixing efficiency over a wide range of Re numbers. To this end, the fluid flow in straight T-shape and serpentine micromixers were analyzed and compared with their counterparts with twist microstructure.

4.1.1. Effect of hydraulic diameters on mixing efficiency of twisted micromixers

Fig. 4 shows the distribution of normalized concentration inside four designs of micromixers as well as the mixing efficiency at outlet (Re = 100). In this figure, the effects of three different hydrodynamic diameters of 100, 300, and 900 μm with a total length of 4.80, 14.58, and 43.6 mm on mixing efficiency were identified. The results demonstrate that the mixing efficiency in twisted micromixers in different hydraulic diameters was dramatically higher than the straight ones,

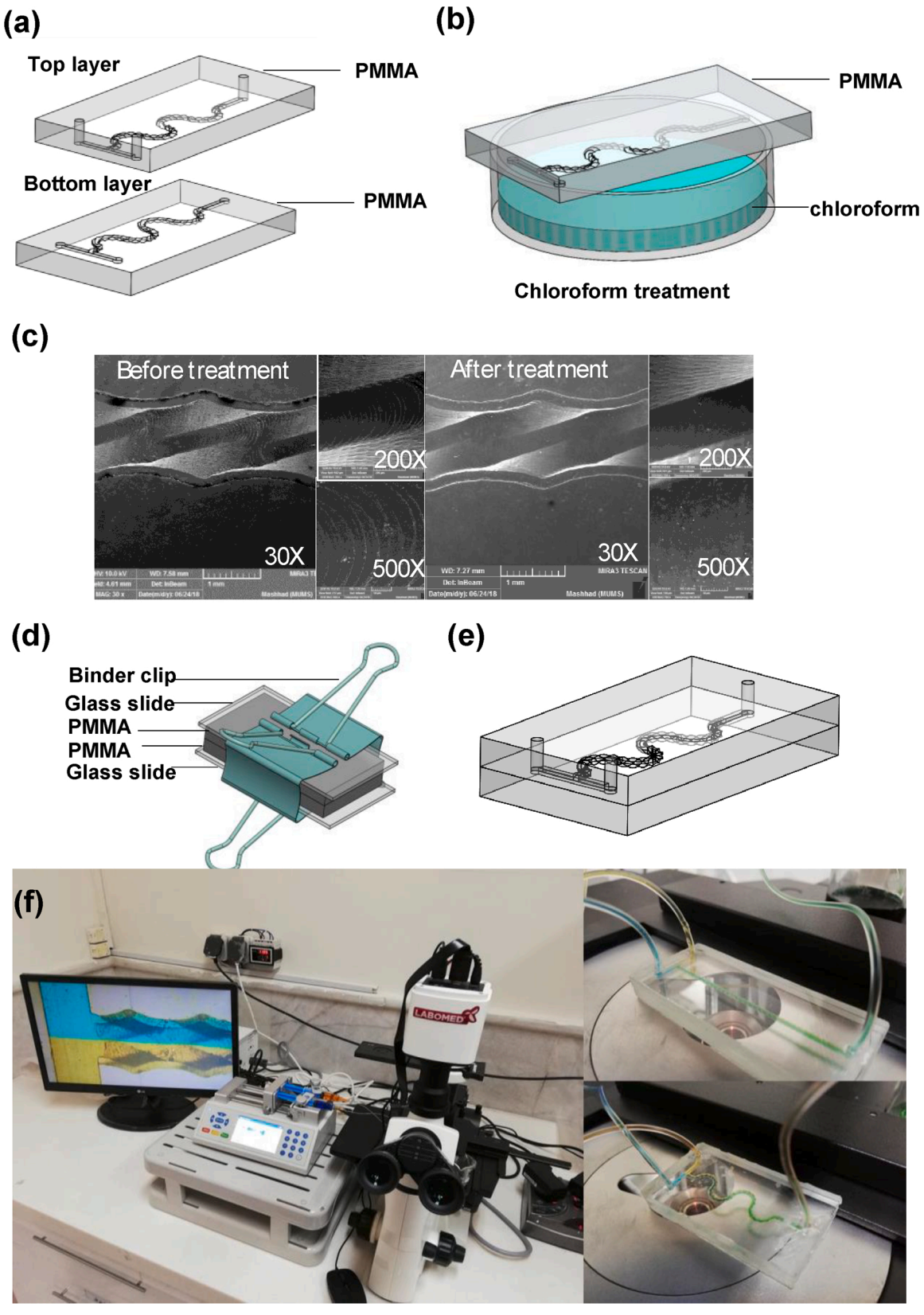

Fig. 3. Schematic illustrations of the fabrication process (a) fabricated layers in PMMA by micromilling; (b) chloroform treatment for 3-4 min at 40 ℃; (c) the SEM images before and after treatment; (d) thermal bonding at 130 ℃ and −80 kPa for 60 min with subsequent cooling to room temperature in 30 min; (d) assembled micromixer; (f) the experimental setup.

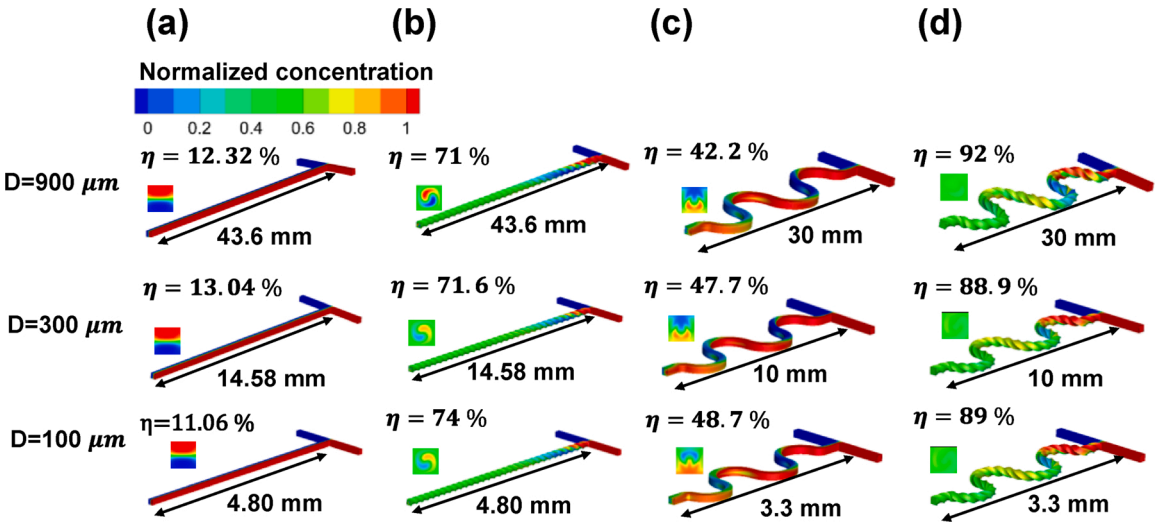

Fig. 4. Normalized concentration of (a) straight, (b) twisted straight, (c) serpentine, (d) twisted serpentine micromixers in different hydrodynamic diameter and micromixer length at Re = 100.

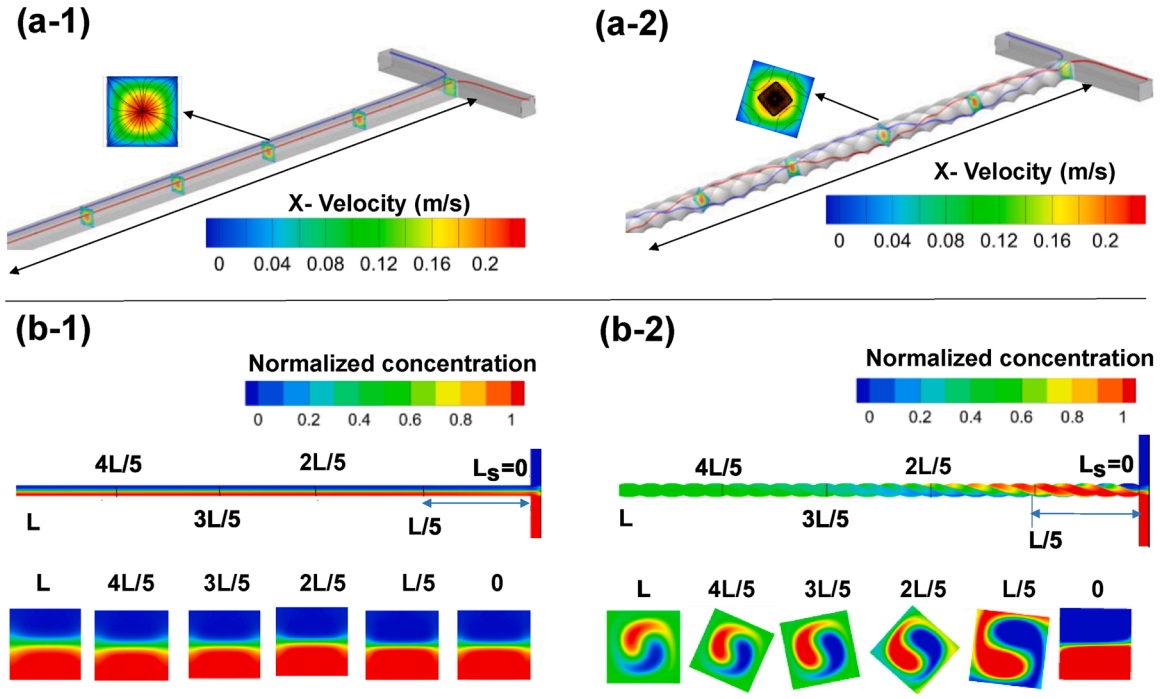

Fig. 5. (a) The x-velocity contours, streamlines and Dean Vortices; (b) the concentration distribution of species in top plane and six different sections of geometries in straight and twisted straight micromixer.

Fig. 4a and b. The mixing efficiency was increased from 11.06% to 74 % for the straight micromixer in $D_h = 100\ \mu m$ and the total length of 4.8 mm that has a seven-fold increase in mixing efficiency. Similarly, in serpentine micromixer, the twist structure could enhance the mixing efficiency from 48.7%–89%, which is a two-fold enhancement. In the twisted serpentine micromixer, the high mixing efficiency could be achieved in the length of 4.8 mm. Hence, the benefit of the proposed twisted structure on the performance of the straight and serpentine micromixers with different hydraulic diameter is highlighted in this figure.

4.1.2. Physics of flow within twisted micromixer with straight and serpentine channel

To comprehend the flow behavior in the twisted straight micromixers, the velocity contours and the streamlines in straight and twisted straight micromixers were depicted in Fig. 5a. The twisted structure induces flow swirling in the microchannel that enhances mixing efficiency, Fig. 5(a-2). Fig. 5b illustrates the distribution of normalized concentration in the top plane of mixing channel and six cross-sections along the mixing channel for straight and twisted straight micromixers with pitch number of 8 and Re number of 100 (2.08 mL/min). The two swirling streams could enhance the mixing process, particularly over channel surface. However, the two streams at the core of the mixing channel experience lower mixing since they are far away from the wall and experience less advection compare to those that exist near the wall. After a specific length in the twisted straight micromixer (about 3 L/5), an increase in the length of the channel had a negligible impact on the mixing efficiency; however, it leads to an increase in the

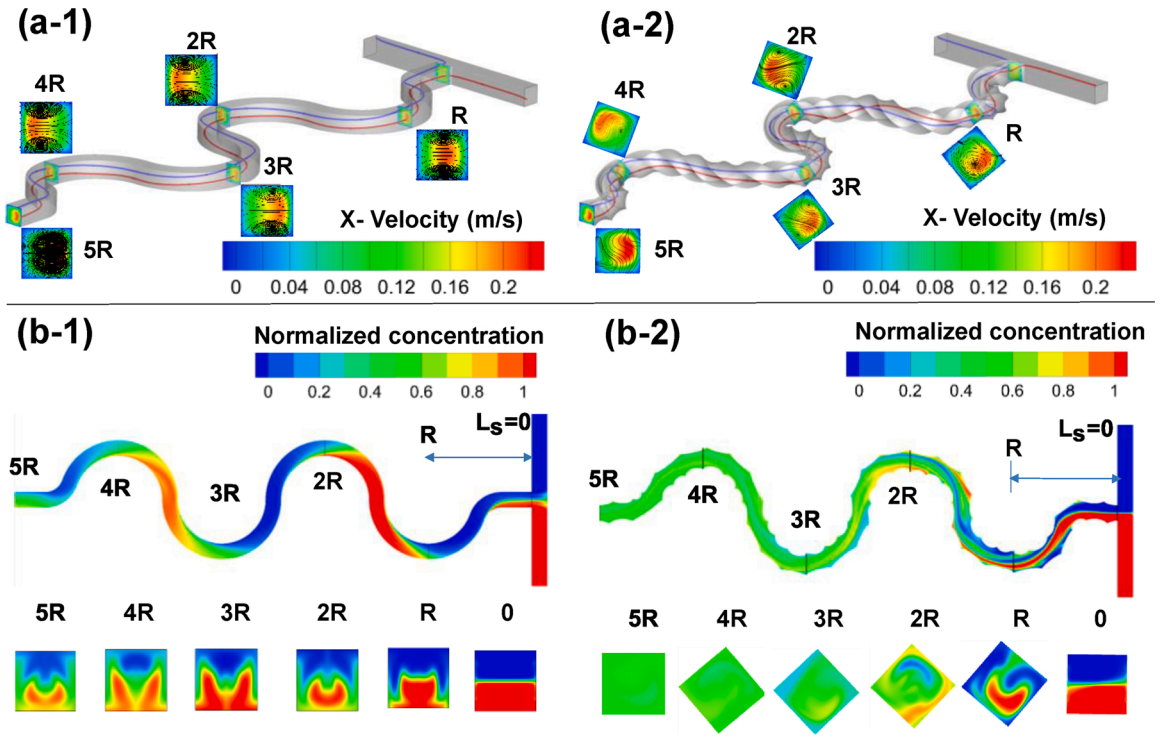

Fig. 6. (a) The x-velocity contours, streamlines and Dean Vortices; (b) the concentration distribution of species in top plane and six different sections of geometries in serpentine and twisted serpentine micromixer.

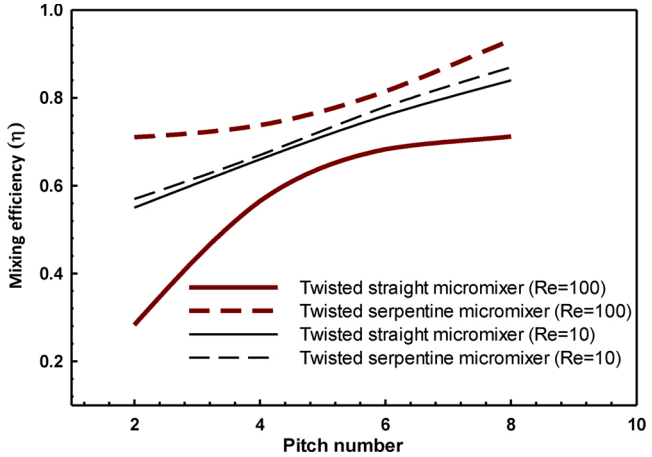

Fig. 7. The variation of mixing efficiency with pitch in the twisted straight and twisted serpentine micromixers at Re = 10 and Re = 100.

pressure drop. Based on this trade-off, 3 L/5 is the efficient length of twisted straight micromixer.

To understand the flow behavior of serpentine and twisted serpentine micromixers, the x-velocity contours, streamline, and Dean vortices in five cross-sections along the length of the channel were plotted, Fig. 6a. Unlike advection in straight micromixer, the chaotic advection produced by Dean Flow enhances transversal transport of species. Introducing a curvature in a serpentine micromixer generates centrifugal force, pulling the fluid, which is close to the inner walls, radially toward the outer walls along the midplane. Simultaneously, the fluid near the outer wall moves inwards along the channel wall. Thus, such fluid movements result in generating the secondary flow across the channel, as well as Dean Vortices in the channel cross-section. The strength of these vortices depends on the Dean number ($De = Re\sqrt{\frac{D}{2R_c}}$) where D is the cross-section diameter and R_c is the radius of curvature of the path. For the present micromixer shown in Fig. 6, Dean Number is equal to 38.72 for Re of 100. In the serpentine micromixer made of repetitive constituted curved segments, the peak velocity position is reversed in subsequent 180-degree bend. Due to the pressure gradient in the outlet section, the maximum velocity of flow shifts toward the inner wall and return to the symmetric profile. Thus, the Dean vortices diminish in the outlet. In contrast, in the twisted serpentine channel, the twisted microstructure causes further instability in the flow and alters the configuration of vortices, Fig. 6(a-2).

The distribution of normalized concentration in the top plane and six cross-sections of serpentine and twisted serpentine micromixers with the pitch number of 8 at Re = 100 (2.08 mL/min) were depicted in Fig. 6b. The induced rotation due to the centrifugal force causes the two-fluid to switch their positions completely which results in enhancement of mixing at the core of the channel, Fig. 6b-1. In comparison with the serpentine micromixer, the twisted serpentine micromixer provided higher mixing efficiency at the core area of the channel and near the channel wall, Fig. 6b-2. This is mainly because of the effects of swirling flow due to the twist microstructure and alternating velocity shift because of the serpentine structure. These synergic effects significantly increase the mixing efficiency.

4.1.3. *Effect of pitch numbers on mixing efficiency*

Fig. 7 illustrates the variation of mixing efficiency with pitch number in twisted straight and twisted serpentine micromixers at Re = 10 and Re = 100. In a twisted straight micromixer at Re of 100, there was a dramatic rise in the mixing efficiency for pitch numbers up to 6; however, at higher pitch numbers, the mixing efficiency reached a plateau. There were about 71.1% and 601% enhancements in the mixing efficiency of twisted straight micromixer compared to the straight micromixer efficiency at Re = 100, at the pitch numbers of 2 and 6, respectively. Combining the two strategies of using (i) curve channel, which generates Dean flow across the channel cross-section, with (ii)

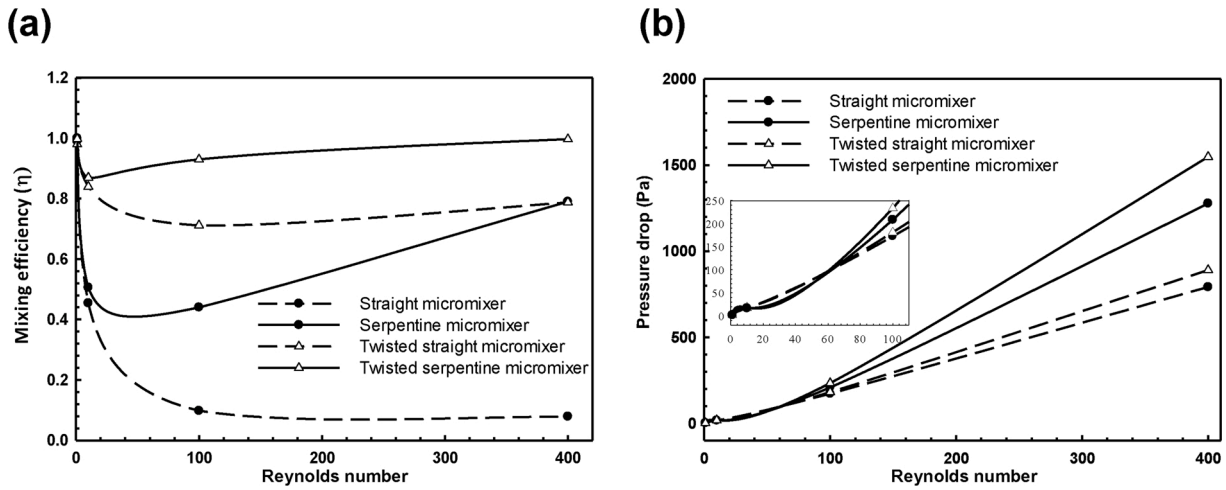

Fig. 8. The variation of (a) mixing efficiency (b) pressure drop versus Re number in four designs of micromixers.

twist microstructure that results in rotating flow along the channel, could increase the mixing efficiency up to nine-fold (93%) at pitch number of 8. It is worth mentioning that the mixing efficiency showed a continual increase versus pitch number for serpentine design. On the other hand, the mixing efficiency illustrated a steady increase versus pitch number at Re number of 10 in both micromixers. Furthermore, the difference of mixing efficiency in low Re number between the twisted serpentine and the twisted straight micromixers was insignificant due to the weak secondary flow generated in the twisted serpentine micromixer design.

4.1.4. *Effect of Reynolds numbers on mixing efficiency*

Fig. 8a shows the effect of Re number on the mixing efficiency of the four micromixers with the same total length, which are straight, twisted straight, serpentine, and twisted serpentine micromixers. For Re = 1, all mixers provided high mixing efficiency almost close to 100% due to the diffusion-dominant mixing mechanism and high residence time of both streams in the mixing channel. However, as the velocity increases, the influence of diffusion on mixing declined gradually, thereby reducing the mixing efficiency. Reshaping the mixer design from straight to serpentine could enhance the mixing efficiency, particularly in high Re numbers (Re number greater than 100) due to the generation of secondary flows. Accordingly, at Re number of 100, mixing efficiency increases from 9% to 44%. However, in low Re number (Re = 10), due to the relatively weak secondary flow (De = 3.87), the mixing efficiency was observed almost the same as the straight micromixer. In other words, there was a wide disparity in mixing efficiency between low Re number of 10 (52%) and a high Re number of 400 (78%).

In the twisted straight micromixer, twist microstructure could enhance the mixing efficiency, particularly in low Re number, unlike the serpentine micromixer. Furthermore, there was a narrower disparity between Re number of 10 (87%) and Re number of 400 (98%), compared to the straight and serpentine micromixer. The minimum mixing efficiency of twisted serpentine micromixer was 87% that was observed at Re = 10. Therefore, this mixer design enabled us to achieve high mixing efficiencies for a wide range of Re numbers. The pressure drop versus Re number was illustrated in Fig. 8b. For all micromixers, the pressure drop increased as the Re number increased. The twisted structure had a minor effect on the pressure drop, especially in low Re number operations. In the twisted straight micromixer, the pressure drop increased up to 12.3% at Re = 400 (890 Pa), which was insignificant compared to the extreme effect of this structure on the mixing efficiency.

Changing the straight micromixer into serpentine micromixer could rise pressure drop from 792.16 Pa to 1277 Pa at Re = 400, that is equivalent to an increase of 61% compared to the straight micromixer in the same flow rate. For the twisted serpentine micromixer at Re numbers of 10 and 100, the pressure drop increased by 7.5% and 35% compared to the straight mixer. For high Re number (Re = 400), the pressure drop was 1547 Pa, 95% higher than straight micromixer in the same flow rate, mainly due to the channel curvatures and ridges on the surface of the channel.

4.2. *Experimental results*

Numerical and experimental results are juxtaposed for a better understanding of the credibility of numerical simulations. Images of flow through the different locations of micromixers (both experimentally and numerically), as well as the normalized concentration from the numerical study, are elucidated in Fig. 9. Careful examination of the figure reveals that at the inlet junction, two streams formed a distinct liquid-liquid interface, represented by two distinct solid colors, with an inter-diffusion zone in green color at the channel centerline. The diffused mixed layer from two streams is discernible by green color, and it became more pronounced as the length increased. Sectional views characterize the level mixing in experimental results. Upon this comparison, numerical results are able to accurately predict experimental results. It was clear that mixing efficiency increased through the channel, and in the outlet section of both micromixers, the green color was observed, indicating the high mixing efficiency.

In this section, to elucidate the advantages of the proposed micromixers, regardless of dimensions and diffusion number, the results are compared to other studies. Fig. 10 revealed that using twist microstructure in serpentine micromixer enabled the mixer to operate in a wide range of Re number with high efficiency compared to other mixer designs available in the literature [8,21,26,39]. It was observed that the micromixers developed by Hossain et al. [39] and Duryodhan et al. [21] had low mixing efficiency in low and intermediate Re number (0.1–270). Based on this figure, the average mixing efficiency of spiral, Tesla, square-wave, and zig-zag micromixer in their studied Re numbers range was calculated to be about 74.2%, 83.5%, 68.6%, and 29.8%, respectively. While the average mixing efficiency in the twisted serpentine micromixer was 94.4% for the Re numbers ranged from 1 to 400. It was clear that the simultaneous use of two designs (twisted wall and serpentine structure) dramatically increased mixing efficiency.

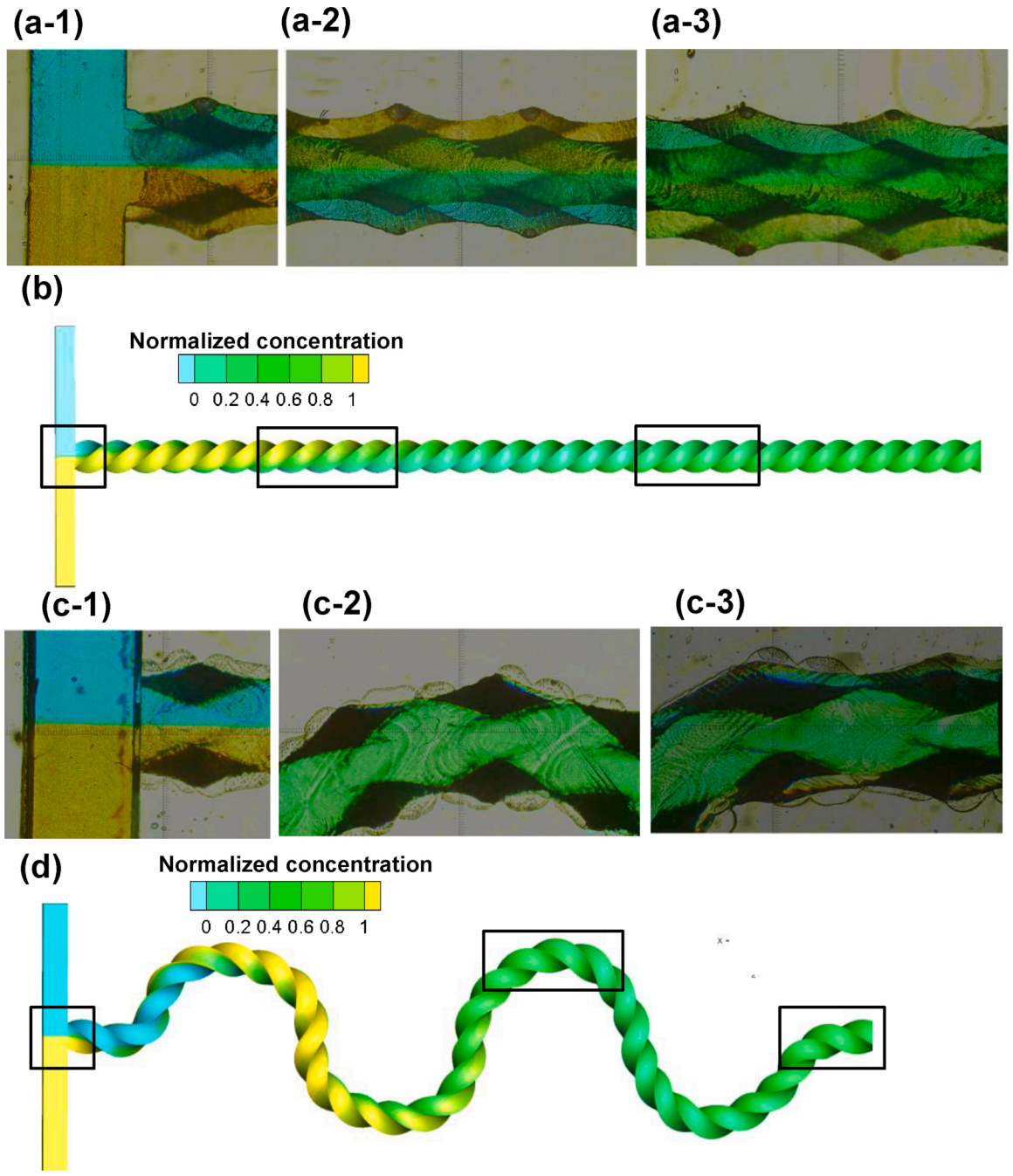

Fig. 9. (a-1), (a-2) and (a-3) the experimental images of inlet, middle and outlet of twisted straight micromixer; (b) the numerical results of normalized concentration; (c-1), (c-2) and (c-3) the experimental images of inlet, middle and outlet of the twisted serpentine micromixer; (d) the numerical results of normalized concentration.

5. Conclusions

In order to improve the mixing efficiency in a wide range of Re numbers, novel micromixers (twisted straight and twisted serpentine micromixer) were introduced and evaluated numerically and experimentally. The 3D microstructure of the micromixers was fabricated in PMMA using a micromilling machine and bonded using thermal diffusion bonding. A numerical model was established to analyze the fluid flow behavior and mixing performance within the proposed twisted microstructures. The effects of pitch, Re number, and channel hydraulic diameter on mixing efficiency and pressure drop were studied numerically. The numerical results revealed that the twisted microstructure enhanced mixing efficiency dramatically, particularly near the wall due to the generating swirl flow through the mixing channel. The effect of twist microstructure on the performance of serpentine micromixer was investigated, and the results illustrated a high mixing efficiency with an average value of 94.4% in a wide range of Re numbers. The mixing length in the twisted serpentine micromixer with a hydraulic diameter of 100 μm was 3.3 mm. Furthermore, the twist structure in straight micromixer increased pressure drop by 12.3%, which was insignificant compared to the extreme effects of this structure on mixing efficiency.

CRediT authorship contribution statement

Shima Akar: Conceptualization, Methodology, Software, Validation, Investigation, Formal analysis, Writing - original draft. **Amin Taheri:**

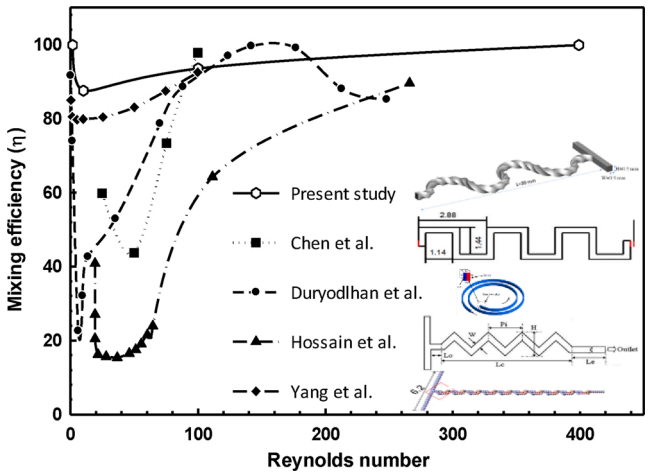

Fig. 10. Comparison of mixing efficiency in different passive micromixers with the proposed twisted serpentine micromixers.

Conceptualization, Investigation, Writing - original draft. **Razavi Bazaz:** Writing - review & editing. **Ebrahimi Warkiani:** Writing - review & editing. **Mousavi Shaegh:** Supervision, Writing - review & editing.

Declaration of Competing Interest

The authors declare that they have no known competing financial interests or personal relationships that could have appeared to influence the work reported in this paper.

Acknowledgment

S.A.M.S. acknowledges financial supports from National Institute for Medical Research Development (NIMAD) under grant number 957144 to conduct this project.

References

[1] W. Li, F. Xia, H. Qin, M. Zhang, W. Li, J. Zhang, Numerical and experimental investigations of micromixing performance and efficiency in a pore-array intensified tube-in-tube microchannel reactor, Chem. Eng. J. 370 (2019) 1350–1365.
[2] N.H. An Le, H. Deng, C. Devendran, N. Akhtar, X. Ma, C. Pouton, H.-K. Chan, A. Neild, T. Alan, Ultrafast star-shaped acoustic micromixer for high throughput nanoparticle synthesis, Lab Chip 20 (2020) 582–591.
[3] P.-C.J.B.J. Chen, An Evaluation of a Real-Time Passive Micromixer to the Performance of a Continuous Flow Type Microfluidic Reactor, vol. 7, 2013, pp. 227–233.
[4] T. Honda, M. Miyazaki, H. Nakamura, H.J.Loa.C. Maeda, Controllable Polymerization of N-Carboxy Anhydrides in a Microreaction System, vol. 5, 2005, pp. 812–818.
[5] J.-N. Kuo, Y.-S.J.M.T. Li, Centrifuge-Based Micromixer with Three-Dimensional Square-Wave Microchannel for Blood Plasma Mixing, vol. 23, 2017, pp. 2343–2354.
[6] V.E. Papadopoulos, I.N. Kefala, G. Kaprou, G. Kokkoris, D. Moschou, G. Papadakis, E. Gizeli, A. Tserepi, A passive micromixer for enzymatic digestion of DNA, Microelectron. Eng. 124 (2014) 42–46.
[7] Y. Wu, L. Li, Y. Mao, L.J. Lee, Static micromixer–Coaxial electrospray synthesis of theranostic lipoplexes, ACS Nano 6 (2012) 2245–2252.
[8] A.-S. Yang, F.-C. Chuang, C.-K. Chen, M.-H. Lee, S.-W. Chen, T.-L. Su, Y.-C.J.C.E.J. Yang, A high-performance micromixer using three-dimensional Tesla structures for bio-applications, Chem. Eng. J. 263 (2015) 444–451.
[9] I. Shah, S.W. Kim, K. Kim, Y.H. Doh, K.H. Choi, Experimental and numerical analysis of Y-shaped split and recombination micro-mixer with different mixing units, Chem. Eng. J. 358 (2019) 691–706.
[10] D. Nouri, A. Zabihi-Hesari, M. Passandideh-Fard, Rapid mixing in micromixers using magnetic field, Sens. Actuators A Phys. 255 (2017) 79–86.
[11] Z. Yang, S. Matsumoto, H. Goto, M. Matsumoto, R. Maeda, Ultrasonic micromixer for microfluidic systems, Sens. Actuators A Phys. 93 (2001) 266–272.
[12] G. Liu, X. Ma, C. Wang, X. Sun, C. Tang, Piezoelectric driven self-circulation micromixer with high frequency vibration, J. Micromechanics Microengineering 28 (2018), 085010.
[13] M. Nazari, S. Rashidi, J.A. Esfahani, Mixing process and mass transfer in a novel design of induced-charge electrokinetic micromixer with a conductive mixing-chamber, Int. Commun. Heat Mass Transf. 108 (2019), 104293.
[14] X. Chen, Z. Wu, Design and numerical simulation of a novel microfluidic electroosmotic micromixer with three electrode pairs, vol. 94, 2019, pp. 1991–1997.
[15] N. Sasaki, T. Kitamori, H.-B. Kim, Fluid Mixing Using AC Electrothermal Flow on Meandering Electrodes in a Microchannel, vol. 33, 2012, pp. 2668–2673.
[16] K.-R. Huang, J.-S. Chang, S.D. Chao, T.-S. Wung, K.-C. Wu, Study of active micromixer driven by electrothermal force, J. Appl. Phys. 51 (2012), 047002.
[17] A.P. Sudarsan, V.M.J.Loa.C. Ugaz, Fluid Mixing in Planar Spiral Microchannels, vol. 6, 2006, pp. 74–82.
[18] N.-T. Nguyen, S.T. Wereley, S.A.M. Shaegh, Fundamentals and Applications of Microfluidics, Artech house, 2019.
[19] W. Ruijin, L. Beiqi, S. Dongdong, Z.J.S. Zefei, A.B. Chemical, Investigation on the splitting-merging passive micromixer based on Baker's transformation, vol. 249, 2017, pp. 395–404.
[20] H.S. Santana, J.L. Silva, O.P. Taranto, Optimization of micromixer with triangular baffles for chemical process in millidevices, Sens. Actuators B Chem. 281 (2019) 191–203.
[21] V. Duryodhan, R. Chatterjee, S.G. Singh, A.J.E.T. Agrawal, F. Science, Mixing in Planar Spiral Microchannel, vol. 89, 2017, pp. 119–127.
[22] P. Garg, J. Picardo, S.J.Po.F. Pushpavanam, Chaotic mixing in a planar, curved channel using periodic slip, Phys. Fluids 27 (2015), 032004.
[23] R.H. Liu, M.A. Stremler, K.V. Sharp, M.G. Olsen, J.G. Santiago, R.J. Adrian, H. Aref, D.J. Beebe, Passive mixing in a three-dimensional serpentine microchannel, J. Microelectromech. Syst. 9 (2000) 190–197.
[24] P. Li, J. Cogswell, M.J.S. Faghri, A.B. Chemical, Design and test of a passive planar labyrinth micromixer for rapid fluid mixing, Sens. Actuators B Chem. 174 (2012) 126–132.
[25] F. Schönfeld, S. Hardt, Simulation of helical flows in microchannels, Aiche J. 50 (2004) 771–778.
[26] X. Chen, T. Li, H. Zeng, Z. Hu, B.J.I.Jo.H. Fu, M. Transfer, Numerical and experimental investigation on micromixers with serpentine microchannels, Int. J. Heat Mass Transf. 98 (2016) 131–140.
[27] K. Liu, Q. Yang, F. Chen, Y. Zhao, X. Meng, C. Shan, Y. Li, Design and analysis of the cross-linked dual helical micromixer for rapid mixing at low Reynolds numbers, Microfluid. Nanofluidics 19 (2015) 169–180.
[28] M. Rafeie, M. Welleweerd, A. Hassanzadeh-Barforoushi, M. Asadnia, W. Olthuis, M. E. Warkiani, An easily fabricated three-dimensional threaded lemniscate-shaped micromixer for a wide range of flow rates, Biomicrofluidics 11 (2017), 014108.
[29] O. Jafari, M. Rahimi, F.H. Kakavandi, Liquid–liquid extraction in twisted micromixers, Chem. Eng. Process. Process. Intensif. 101 (2016) 33–40.
[30] D.J. Kang, Effects of channel wall twisting on the mixing in a T-Shaped micro-channel, Micromachines (Basel) 11 (2020) 26.
[31] P.V. Danckwerts, The definition and measurement of some characteristics of mixtures, Appl. Sci. Res. Section A 3 (1952) 279–296.
[32] J.P. Van Doormaal, G.D. Raithby, Enhancements of the simple method for predicting incompressible fluid flows, Numer. Heat Transf. 7 (1984) 147–163.
[33] C.A. Cortes-Quiroz, A. Azarbadegan, M. Zangeneh, Evaluation of flow characteristics that give higher mixing performance in the 3-D T-mixer versus the typical T-mixer, Sens. Actuators B Chem. 202 (2014) 1209–1219.
[34] S.A.M. Shaegh, A. Pourmand, M. Nabavinia, H. Avci, A. Tamayol, P. Mostafalu, H. B. Ghavifekr, E.N. Aghdam, M.R. Dokmeci, A. Khademhosseini, Rapid prototyping of whole-thermoplastic microfluidics with built-in microvalves using laser ablation and thermal fusion bonding, Sens. Actuators B Chem. 255 (2018) 100–109.
[35] A. Pourmand, S.A.M. Shaegh, H.B. Ghavifekr, E.N. Aghdam, M.R. Dokmeci, A. Khademhosseini, Y.S. Zhang, Fabrication of whole-thermoplastic normally closed microvalve, micro check valve, and micropump, Sens. Actuators B Chem. 262 (2018) 625–636.
[36] A. Banejad, M. Passandideh-Fard, H. Niknam, M.J.M. Hosseini, S.A.M. Shaegh, Design, fabrication and experimental characterization of whole-thermoplastic microvalves and micropumps having micromilled liquid channels of rectangular and half-elliptical cross-sections, Sens. Actuators A Phys. 301 (2020), 111713.
[37] A. Banejad, S.A. Mousavi Shaegh, E. Ramezani-Fard, P. Seifi, M. Passandideh-Fard, on the performance analysis of gas-actuated peristaltic micropumps, Sens. Actuators A Phys. 315 (2020), 112242.
[38] R.Q. Frazer, R.T. Byron, P.B. Osborne, K.P. West, PMMA: an essential material in medicine and dentistry, J. Long. Eff. Med. Implants 15 (2005).
[39] S. Hossain, M.A. Ansari, K.-Y. Kim, Evaluation of the mixing performance of three passive micromixers, Chem. Eng. J. 150 (2009) 492–501.